

## Spiral Turbulence and Phase Dynamics

John J. Hegseth, C. David Andereck, F. Hayot, and Y. Pomeau<sup>(a)</sup>

*Department of Physics, Ohio State University, 174 West 18th Avenue, Columbus, Ohio 43210*

(Received 22 August 1988)

Hysteretic spiral turbulence is a remarkable phenomenon of coexistence of turbulent and laminar domains in Taylor-Couette flow. We observe and measure for the first time a nonuniform pitch in long geometries and its dependence on boundary conditions at the cylinder ends, and we explain these results within the framework of phase dynamics. We also discuss the influence of secondary flow on the azimuthal width of the spiral.

PACS numbers: 47.20.-k, 47.30.+s

Spiral turbulence—the coexistence of laminar and turbulent spiral regions in Taylor-Couette flow—is highlighted by Feynman<sup>1</sup> as an example of the richness of phenomena described by the Navier-Stokes equations (see Fig. 1). Spiral turbulence has been extensively studied by Coles<sup>3</sup> and its existence region for a particular geometry mapped out in the  $(R_o, R_i)$  plane of Taylor-Couette flow between concentric rotating cylinders. Here  $R_o$  and  $R_i$  are proportional to the angular velocities  $\Omega_o$  and  $\Omega_i$  of the outer and inner cylinder, respectively [ $R_o = b(b-a)\Omega_o/\nu$  and  $R_i = a(b-a)\Omega_i/\nu$ , where  $a$  is the radius of the inner and  $b$  is the radius of the outer cylinder, and  $\nu$  is the kinematic viscosity]. Subsequently Van Atta,<sup>4</sup> at one point in the parameter space, measured the pitch of the spiral and mapped its profile in a plane perpendicular to the cylinder axes.

Spiral turbulence is particularly interesting among all fluid instabilities, because it mixes short scale (or microscale) turbulence and a well ordered structure at large scales. It is the prototype of the “coherent structures” of great interest in fluid mechanics in recent years.<sup>5</sup> In this Letter we report new measurements of spiral turbulence, in particular of the spiral pitch, for different boundary conditions, and propose a theoretical approach in the spirit of Feynman<sup>1</sup> “to find the qualitative content of the Navier-Stokes equations.” The novel observation that the pitch varies along the axis fits well into a phase dynamics approach, which—we believe—is here applied for the first time to a situation with sustained microscale turbulence. In addition the well-known<sup>3,4</sup> observation that the turbulent spiral is of finite azimuthal width, will be explained as resulting from the subcritical character of the flow and its boundedness in the azimuthal direction.

It is important to stress the subcritical character of the laminar-spiral turbulence transition, which leads to large hysteretic effects.<sup>2,3</sup> As shown by one of us,<sup>6</sup> subcritical instabilities in general should lead to expanding or contracting turbulent domains in laminar flow. For the finite Taylor-Couette system, this cannot be the whole story. In fact, large-scale Poiseuille flow in the laminar region is generated by Reynolds stress in the turbulent

region. The case of weakly inclined, supercritical Taylor vortices was worked out by Hall,<sup>7</sup> who completed previous work<sup>8</sup> on amplitude equations. In Hall's work<sup>7</sup> the backflow is proportional to an integral over azimuthal angle involving the square of the amplitude, which itself is proportional to the Reynolds stress.<sup>9</sup> The theory for the subcritical case has not yet been worked out, however; the same basic mechanism must be at work, and this allows for a qualitative understanding. The backflow

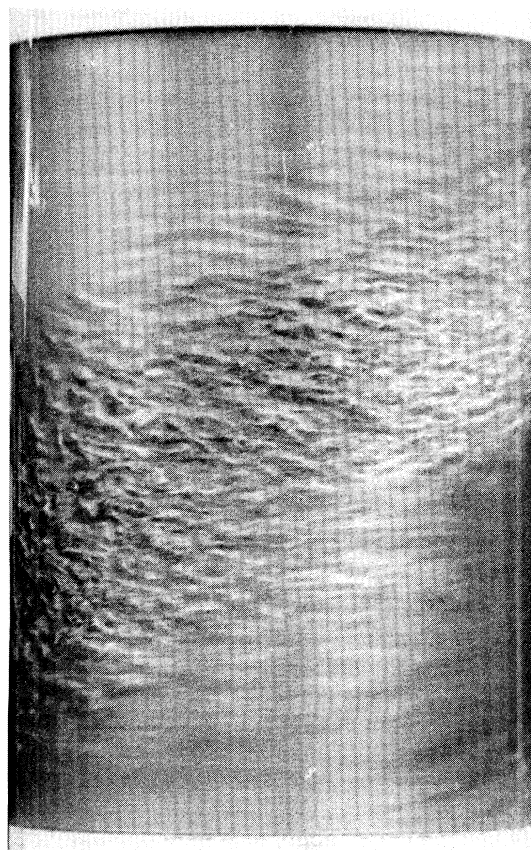


FIG. 1. Spiral turbulence for fixed upper and lower boundaries, aspect ratio 30,  $R_o = -3000$ ,  $R_i = 700$  (from Ref. 2).

counteracts the velocity of expansion of the turbulent spot until the latter stops. The matching of azimuthal Reynolds numbers (the relevant length being the azimuthal width of each region) for laminar and turbulent flow (assumed to have the same average velocity) leads at onset to roughly equal azimuthal width of each region, up to the mismatch between molecular and turbulent viscosities in the respective regions.

The experimental apparatus used here has been largely described in a previous paper.<sup>10</sup> In brief, the geometric parameters of our system are the radius ratio  $a/b=0.882$  and the aspect ratio  $\Gamma=L/(b-a)$ , which can be as large as 73. The cylinder speeds were controlled by Compumotor stepping motors with a rotation-rate precision of  $\pm 0.01\%$ . The working fluid in all cases was distilled water, with visualization of the pattern accomplished by the addition of 1% by volume Kalliroscope polymeric flakes. With a free upper surface the fluid level may be changed continuously while the cylinders rotate. Perturbation experiments in the hysteretic regime were carried out by our injecting fluid into completely laminar flow through a small hole (0.15 cm diam) in the side of the Plexiglas outer cylinder. Approximately  $0.1 \text{ cm}^3$  of fluid is injected over a time of less than 0.03 sec, while monitoring the visualized flow with a television camera mounted on a rotating table. The angular velocity of the table was set equal to the expected velocity of the turbulent spots (and ultimately the turbulent spiral). Measurements of the pitch were made by use of a multiple detector reflectance technique. At two points along the axis, light from He-Ne lasers is focused on the fluid and the reflected light detected by photodiodes, the output of which is digitized and sent to our PDP-11/73 computer for analysis. The time delay between the two signals, together with the distance between the detectors, yields the pitch.

We have followed the azimuthal and axial expansions of a spot created at the midpoint of the cylinder in the manner described above. The spot created expands initially much faster ( $\sim 2$  times) in the azimuthal direction than in the axial one as shown in Fig. 2. The azimuthal expansion stops as soon as about half of the perimeter length is reached, i.e., from our point of view as soon as there is sufficient backflow. The spot then breaks into two spots in the axial direction, which propagate axially and azimuthally, their width being always approximately that of the final spiral. These spots may then undergo further splitting and subsequent growth. The different pieces eventually connect and construct a spiral. The presence of axial propagation shows that the backflow has in fact a complex three-dimensional structure.

Spiral turbulence is found over a wide range of  $R_o$  and  $R_i$ . We limited our detailed survey to the hysteretic regime. We have found that for  $\Gamma=73$  persistent spirals occurred only for  $R_o > -4000$ , and that at  $R_o = -8000$  no large scale organized structure was apparent. In this

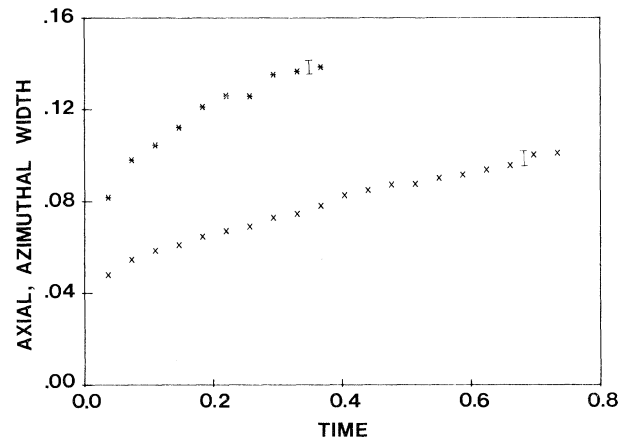


FIG. 2. Axial ( $\times$ ) and azimuthal ( $*$ ) widths of turbulent spots for  $R_o = -3000$ ,  $R_i = 770$ . The widths are scaled by the average perimeter length of 35.3 cm, and the time by the outer cylinder period of 0.91 sec. Fits to the first seven points in each case yields initial front velocities of 1.78 cm/sec for the axial case and 3.86 cm/sec for the azimuthal case. Representative error bars are shown for each case.

case a “broken” spiral pattern is found, i.e., the pattern may be locally a spiral, but the helicity changes over an axial distance of the order of the cylinder diameters. Some regions may not show even local spirals, just turbulent patches. This same incoherent state is found with either free or rigid upper boundary. A simple spiral pattern does not emerge until the aspect ratio is lowered to  $\approx 28$ . Measurements on the simple spirals at large aspect ratio were therefore confined to  $R_o \approx -3000$ . As shown in Fig. 3 these spirals were *always* observed to have a pitch that varied with axial position. We take first the case in which the top and bottom boundaries are rigid and move with the outer cylinder. If the outer cylinder, as viewed from *above*, rotates clockwise, then a right-handed spiral would have a *lower* pitch near the *bottom* of the cylinder than near the *top*, while a left-handed spiral has a *larger* pitch near the bottom than at the top. If the outer cylinder rotates counterclockwise, then, consistent with the first observations, a right-handed spiral would have a *lower* pitch at the *top* of the cylinder than at the bottom, while a left-handed spiral would have a *larger* pitch at the top than at the bottom. In other words, the pitch is lower near the end away from which the spiral appears to be moving. The average pitch depends only weakly on  $R_i$ . Its value is compatible with that measured previously.<sup>4</sup> With a free upper surface the picture changes dramatically. For a counterclockwise rotation of the outer cylinder, a right-handed spiral looks much the same as for the rigid-rigid boundary condition case, while a left-handed spiral has a much lower average pitch. In the former case the spiral wraps around the cylinder approximately twice, while in the

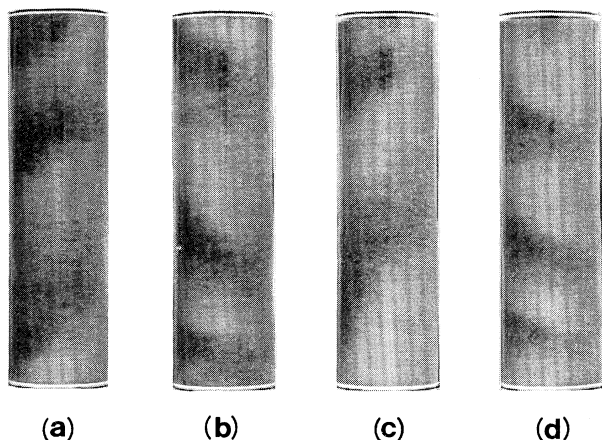


FIG. 3. Spiral turbulence with  $\Gamma \cong 73$ ,  $R_o = -3000$ ,  $R_i = 950$ , and outer cylinder rotating counterclockwise viewed from above. The turbulent band always turns in the direction of rotation of the outer cylinder. (a) and (b) have rigid upper boundaries, (c) and (d) have free upper boundaries. In (a) and (c) the spirals propagate downward and have lower pitch at the top. In (b) and (d) the spirals propagate upward and have lower pitch at the bottom. There is a substantial average pitch difference between (c) and (d) as discussed in the text. Typical pitch angles for case (b) are  $19^\circ \pm 1^\circ$  at the bottom and  $44^\circ \pm 6^\circ$  at the top, while for (d) they are  $16^\circ \pm 0.5^\circ$  at the bottom and  $29^\circ \pm 2^\circ$  at the top.

latter case it wraps around 3 times. In all of these cases the spiral pitch persisted over many hours of observation and was reproducible from run to run.

We shall now attempt a simple phase-dynamics approach to describe the observed pitch of the turbulent spiral and its variations, compatible with the symmetries of the problem.

Let  $\varphi(z, t)$  be the mean azimuthal position of the spiral at height  $z$  and time  $t$ . We treat  $\varphi$  as a real quantity, its periodicity does not matter for the present purpose. The quantity  $\varphi$  is a phase in the sense that a uniform shift of  $\varphi$  has no dynamical effect, because of the axisymmetry of Taylor-Couette flow. The simplest possible form of a phase equation then takes the same form as that considered by Pocheau *et al.*,<sup>11</sup> for representing the effect of transverse flow on Rayleigh-Benard roll structure, namely,

$$\varphi_t + v\varphi_z = D\varphi_{zz}. \quad (1)$$

We shall postpone considerations of boundary conditions, and note that Eq. (1) has a family of solutions

$$\varphi = w(vt - z)/v + \Phi(z), \quad (2)$$

where  $w$  is a constant of integration and  $v$  is the apparent axial velocity of the spiral in the laboratory frame.  $\Phi(z)$  is considered below. The value of the pitch is undetermined, as is the wave number of the Rayleigh-Benard rolls in the phase equation of Ref. 11. The absolute

value of the pitch should be allowed to vary in a band, as the roll wave number. This can be taken into account<sup>11</sup> by the introduction of a pitch dependence in  $D$  [cf. (1)]. We shall neglect this in our simple approach, as well as any velocity dependence on pitch. The function  $\Phi(z)$  in (2) is the solution of  $v\Phi_z = D\Phi_{zz}$  and thus of the form

$$\Phi(z) = \varphi_0 \exp(vz/D). \quad (3)$$

The only boundary conditions compatible with phase invariance are  $\varphi_z = \alpha$  at one end (say  $z=0$ ) and  $\varphi_z = \beta$  at the other end ( $z=L$ ). Parameters  $\alpha$  and  $\beta$ , which describe the locally imposed pitch, could be computed in principle within the framework of a complete amplitude equation. Similar coefficients have been calculated by Cross<sup>12</sup> in a different context. Those terms should take into account the interaction between the Ekman layer and the finite amplitude solution.

We do not expect  $\alpha$  and  $\beta$  to be the same, because of the structure of turbulence within the spiral. The observed splitting of a spot into two, one moving upwards, one downwards, reflects itself in the end in the existence of spirals of either helicity. It corresponds to a spontaneous axial symmetry breaking, which should be associated with a difference in the internal structure of the spots, made of progressive finite amplitude waves moving axially in either direction. As the fluid outside the spiral is linearly stable against those waves, they only propagate within spiral boundaries, being emitted at one side and absorbed at the other. This view is consistent with the observed asymmetry between leading and trailing edges of the spiral azimuthal profile.<sup>4</sup> Consequently, waves are emitted at one end of the spiral and absorbed at the other, which leads to  $\alpha$  being different from  $\beta$ . A full picture would need an extension of the results in Ref. 6 to complex amplitudes of progressive waves.

We note that the same symmetries as above would be present for spiraling Taylor vortices.<sup>7,8</sup> There too the pitch would be nonuniform, at least for large aspect ratios. On the other hand, the subtle dependence of wavelength (here pitch) upon boundary conditions<sup>13</sup> for steady structures such as Rayleigh-Benard rolls near threshold, does not seem to be relevant for inclined Taylor vortices. This is because their phase is always increasing or decreasing when measured at the boundary. Thus this phase cannot be taken as a relevant constant parameter for constraining the wavelength of the structure. The general solution of Eq. (2) is thus

$$\varphi(z, t) = w(vt - z)/v + \varphi_0 \exp(vz/D). \quad (4)$$

Here  $\varphi_0$  and  $w$  are determined by boundary conditions at  $z=0$  and  $z=L$ ,

$$\varphi_0 = \frac{D}{v} \frac{\alpha - \beta}{1 - \exp(vL/D)}, \quad \frac{w}{v} = \varphi_0 \frac{v}{D} - \alpha. \quad (5)$$

There is then a continuous variation of the pitch  $\varphi_z$  between  $\alpha$  and  $\beta$ . The experimental results show that  $\alpha \neq \beta$ ,

generically. If  $\alpha = \beta$ , then from (5),  $\varphi_0 = 0$  and one obtains the solution of constant pitch  $\varphi(z, t) = -\alpha(vt - z)$ . We note that Eq. (1) is invariant under the symmetry

$$\begin{pmatrix} z \rightarrow -z \\ v \rightarrow -v \end{pmatrix},$$

which relates two possible spirals of opposite helicity. This, however, also interchanges boundary conditions and therefore a spiral that in one helicity is compressed at the bottom and expanded at the top shows the opposite behavior in the other helicity. These features are evident in the experimental data.

However, once the symmetry between bottom and top is broken, as in the case when the top interface is a free surface and the bottom one rigid, there is no reason based on symmetry that the two spirals of opposite helicity are related. For the free-rigid case, this is what the data show. The data moreover show that for one of the helicities the pitch is relatively insensitive to whether the upper surface is rigid or free.

Phase dynamics thus provides a simple framework in which to discuss the pitch of spiral turbulence, its axial variation, and dependence on boundary conditions.

A final remark is the following: As reported above, at  $R_o = -8000$  a simple spiral pattern only emerges at low aspect ratio. There is an apparent contradiction between this result and the stable spiral solutions of Eq. (1), which exist at any cylinder length  $L$ . However, the greater  $L$ , the less stable the spiral becomes, because the least stable perturbation decays as  $\exp(-D\pi^2/L^2)t$ . We conjecture that for large aspect ratio the spiral becomes unstable against a secondary instability, not included in the phase dynamics approach, and which involves coupling with complex secondary flow.<sup>14</sup> This conjecture is reinforced by the fact that the typical correlation length for a broken turbulent spiral is of the order of the cylinder diameter, which also characterizes the large scale flows.

This work was supported by the Office of Naval Research (Contract No. N00014-86-K-0071), the

Department of Energy (Contract No. DE-FG02-88ER13916.A000), and by a CNRS Programme International de Coopération Scientifique.

<sup>(a)</sup>Permanent address: Laboratoire de Physique Statistique, associé CNRS, Ecole Normale Supérieure, 24, rue Lhomond, 75005 Paris, France.

<sup>1</sup>R. P. Feynman, *Lecture Notes in Physics* (Addison-Wesley, Reading, MA, 1964), Vol. 2.

<sup>2</sup>C. D. Andereck, S. S. Liu, and H. L. Swinney, *J. Fluid Mech.* **164**, 155 (1986).

<sup>3</sup>D. Coles, *J. Fluid Mech.* **21**, 385 (1965).

<sup>4</sup>C. W. Van Atta, *J. Fluid Mech.* **25**, 495 (1966). See also D. Coles and C. W. Van Atta, *Phys. Fluids* **10**, S120 (1967); D. Coles and C. W. Van Atta, *AIAA J.* **4**, 1969 (1966).

<sup>5</sup>A. K. M. F. Hussein, *Phys. Fluids* **26**, 2816 (1983), and references therein.

<sup>6</sup>Y. Pomeau, *Physica (Amsterdam) D* **23**, 1 (1986), and in *Proceedings of the Conference on Fluctuations and Instabilities, Chile, 1987*, edited by E. Tirapegui and L. Villaroel (Reidel, Dordrecht, to be published).

<sup>7</sup>P. Hall, *Phys. Rev. A* **29**, 2921 (1984).

<sup>8</sup>P. Tabeling, *J. Phys. Paris, Lett.* **44**, L665 (1983); H. Brand and M. C. Cross, *Phys. Rev. A* **27**, 1237 (1983).

<sup>9</sup>A. Davey, L. M. Hocking, and K. Stewartson, *J. Fluid Mech.* **63**, 529 (1974).

<sup>10</sup>G. W. Baxter and C. D. Andereck, *Phys. Rev. Lett.* **57**, 3046 (1986).

<sup>11</sup>A. Pocheau, V. Croquette, P. Le Gal, and C. Poitou, *Europhys. Lett.* **3**, 915 (1987).

<sup>12</sup>M. C. Cross, *Phys. Rev. Lett.* **57**, 2935 (1986).

<sup>13</sup>Y. Pomeau and S. Zaleski, *J. Phys. Paris, Lett.* **44**, 135 (1983); M. C. Cross, P. G. Daniels, P. C. Hohenberg, and E. D. Siggia, *J. Fluid Mech.* **127**, 155 (1983).

<sup>14</sup>The explicit coupling between large scale flow and phase dynamics in a Rayleigh-Benard system at low to moderate Prandtl number has been considered by A. Pocheau, *C.R. Acad. Sci.* **306**, 331 (1988), and by A. C. Newell, in *Propagation in Nonequilibrium Systems*, edited by J. E. Wesfreid, H. R. Brand, P. Manneville, G. Albinet, and N. Boccara (Springer-Verlag, Berlin, 1988), p. 122.

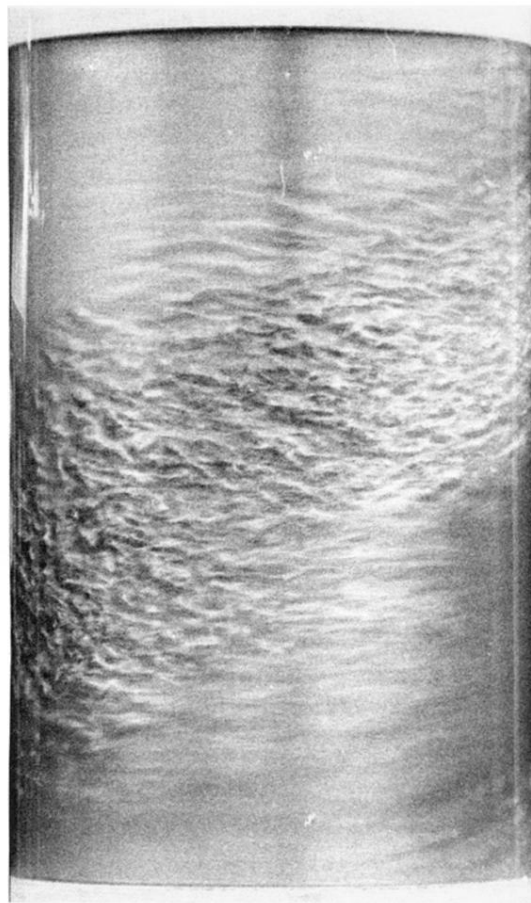


FIG. 1. Spiral turbulence for fixed upper and lower boundaries, aspect ratio 30,  $R_o = -3000$ ,  $R_i = 700$  (from Ref. 2).

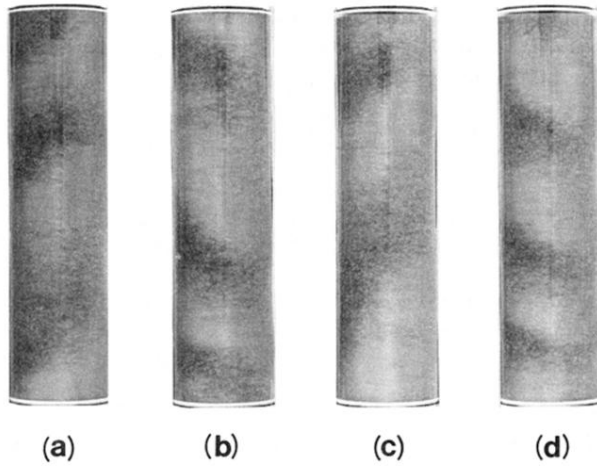


FIG. 3. Spiral turbulence with  $\Gamma \cong 73$ ,  $R_o = -3000$ ,  $R_i = 950$ , and outer cylinder rotating counterclockwise viewed from above. The turbulent band always turns in the direction of rotation of the outer cylinder. (a) and (b) have rigid upper boundaries, (c) and (d) have free upper boundaries. In (a) and (c) the spirals propagate downward and have lower pitch at the top. In (b) and (d) the spirals propagate upward and have lower pitch at the bottom. There is a substantial average pitch difference between (c) and (d) as discussed in the text. Typical pitch angles for case (b) are  $19^\circ \pm 1^\circ$  at the bottom and  $44^\circ \pm 6^\circ$  at the top, while for (d) they are  $16^\circ \pm 0.5^\circ$  at the bottom and  $29^\circ \pm 2^\circ$  at the top.